

## Evidence for the Ir(100) Surface Reconstruction by Field-Ion Microscopy

J. Witt and K. Müller

*Lehrstuhl für Festkörperphysik, Universität Erlangen-Nürnberg, D-8520 Erlangen, Federal Republic of Germany*

(Received 7 April 1986)

The reconstruction of the Ir(100) surface as well as the transition of the regular bulklike structure into the reconstructed phase by thermal activation at  $T > 800$  K has been observed in a field-ion microscope. The field-ion microscope image of the thermally stable reconstructed surface supports the rippled quasihexagonal structure model for Ir(100)( $1 \times 5$ ) already developed from LEED structure analyses.

PACS numbers: 68.35.-p, 61.16.Fk

Some low-index single-crystal surfaces are known to form reconstructed surface structures. As a consequence of broken bonds and missing nearest neighbors the atomic arrangement at the surface differs from that of the corresponding volume net plane. Various examples of this phenomenon have been investigated by LEED and other surface-sensitive methods. Field-ion microscopy (FIM), however, has so far contributed comparatively little to the phenomenon of reconstruction, except for the work of Melmed *et al.* on W(100),<sup>1</sup> and Kellogg on Pt(110).<sup>2</sup> Nevertheless, more results from direct observations in real space are highly desirable. Ir(100) is one of the well-known reconstructing surfaces. Its ( $1 \times 1$ ) bulklike surface structure exists as a metastable phase which converts irreversibly by thermal activation at  $T > 800$  K into the stable reconstructed ( $1 \times 5$ ) structure.<sup>3</sup> Surface models for the latter phase have been developed by independent and elaborate LEED analyses<sup>4</sup> which agree in all essential details.

The present work was stimulated by the fact that no previous FIM studies on Ir tips had shown any indication of a modified (100) surface structure. We report for the first time the direct observation of a stable Ir(100) superstructure as well as its transition to the ( $1 \times 1$ ) phase in the field-ion microscope. The experiments were performed in an UHV stainless-steel chamber with a residual gas pressure of  $10^{-8}$  Pa. Initially the sample was cleaned from possible contaminants by heat treatment at 1500 K, Ne sputtering, and subsequent field evaporation. Beginning with the regular FIM image of an Ir tip at  $T = 20$  K, the appearance of the (100) terrace changes after a heating interval ( $T = 1500$  K) of a few seconds during which the imaging field was cut off. Rows of atoms appear, like in Fig. 1 [similar formation of Ir-atom rows on W(110) has been reported by Bassett<sup>5</sup>]. Atoms at the border of the terrace are well resolved so that the interatomic distance ( $a$ ) within the rows and the distance of adjacent rows ( $r$ ) can be determined. Their ratio is  $r/a = 1.6$ .

For a more detailed analysis of the FIM image a video system was applied which allows us to take intensity profiles along any chosen direction. Therefore the FIM image is viewed directly by a video camera whose signal is transferred to a LSI 11 processor.<sup>6</sup> After selection of the area of interest (here a narrow slit of the total image along a certain direction) the system displays (on line) the desired intensity profiles. Figure 2 shows sets of profiles taken parallel as well as perpendicular to the rows of atoms observed. Again nearest-neighbor distances ( $a$ ) and row distances ( $r$ ) can be measured. The ratio of their mean values turns out to be  $\bar{r}/\bar{a} = 1.6 \pm 0.1$ , which matches the direct observation in Fig. 1.

We now come back to the surface model developed by LEED analyses for the Ir(100)( $1 \times 5$ ) reconstruc-

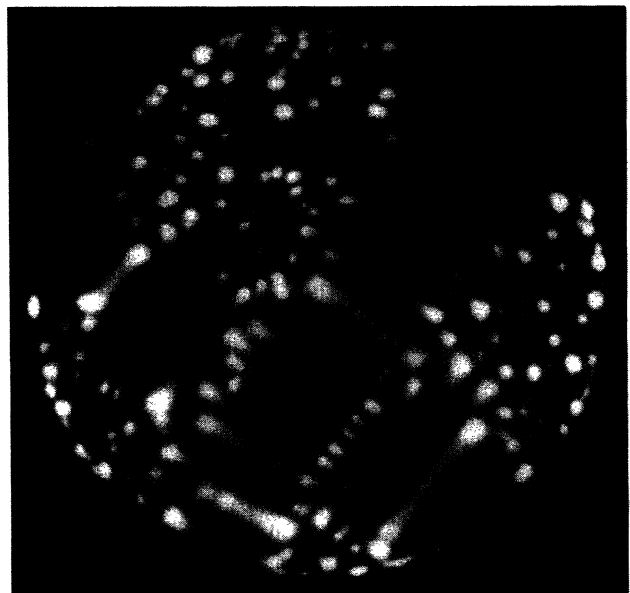


FIG. 1. FIM image of the Ir(100) plane after flashing of the tip to about 1500 K.

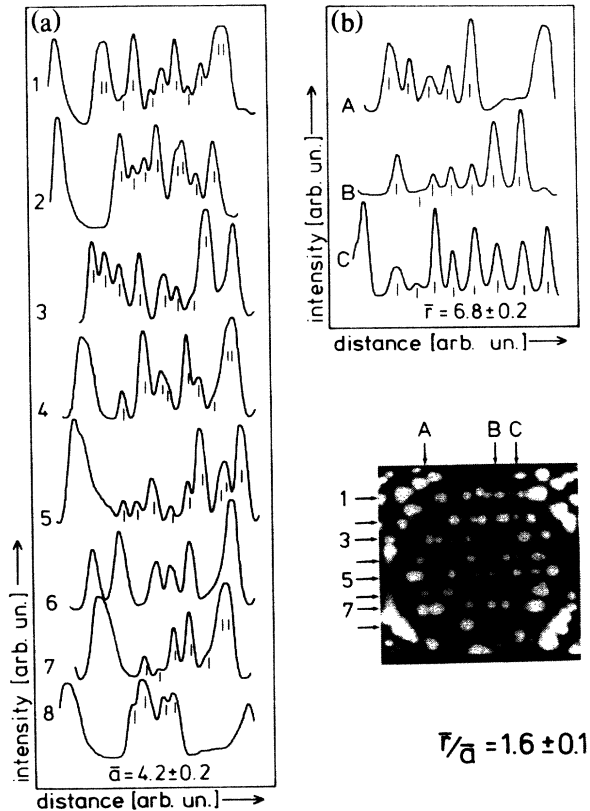


FIG. 2. Intensity profiles along (left-hand panel) and across (right-hand panel) rows taken from the FIM image shown at the lower right.

tion which is shown in Fig. 3. It consists of a quasi-hexagonal surface whose considerable layer rippling of  $\Delta = 0.5 \text{ \AA}$  can best be seen in the side view. This layer rests on an undisturbed bulklike net plane with fourfold symmetry. Every second row of atoms ( $\alpha = 1, 3, 5, \dots$ ) sticks further out of the surface than those in between ( $\beta = 2, 4, 6, \dots$ ). The ratio of the distance ( $r$ ) of rows  $\alpha$  to the interatomic distance ( $a$ ) within the rows is  $r/a = \frac{5}{3}$ . If we include in Fig. 3 a line (trace of a plane) of constant mean distance from the surface at which the imaging atoms ionize, then it becomes qualitatively apparent that the tunneling probability, decaying exponentially with distance, must be higher above rows  $\alpha$  than above rows  $\beta$ . (A Jeffreys-Wentzel-Kramers-Brillouin calculation of the tunneling probability, after Homeier and Kingham<sup>7</sup> and Witt and Müller,<sup>7</sup> predicts an intensity ratio for the images of rows  $\alpha$  and  $\beta$  of 4:1.) With the assumption that the displayed FIM image shows preferentially the more protruding rows  $\alpha$ , the observation is in excellent agreement with the surface model developed from LEED experiments.

Inspection of Fig. 1 might also suggest a model of

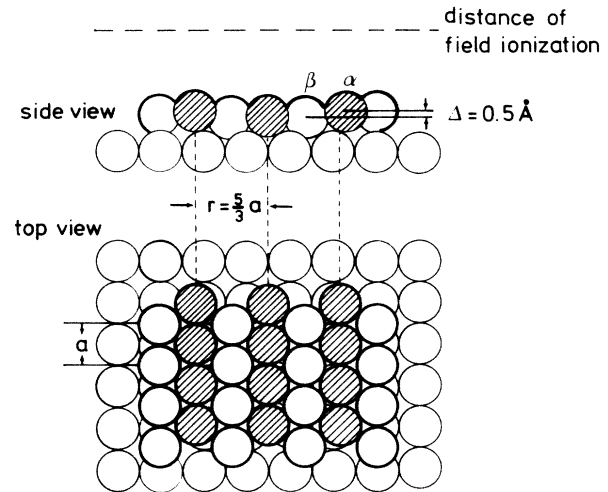


FIG. 3. Structure model for the reconstructed Ir(100) ( $1 \times 5$ ) surface developed from LEED structure analyses. Upper part, side view, showing the corrugation of the topmost layer; lower part, top view, showing the unit mesh of the ( $1 \times 5$ ) superstructures.

the reconstructed surface which contains regularly spaced rows of vacancies in the topmost layer. Models of this kind have indeed been suggested for Ir(100) but have been turned down in the course of LEED structure analyses.<sup>8</sup> All of these models can again be disregarded because neither one of their characteristic vacancy row distances agrees with the FIM observation. Single atoms of valley rows  $\beta$  are sometimes imaged at the terrace edge.

An alternative interpretation would regard the actually imaged atoms as adatoms decorating the troughs of an underlying reconstructed surface. If so, the observation would again be indicative of the reconstruction model, in this case supporting an adsorbate. Field evaporation of the top layer as shown in Fig. 4, however, reveals a substrate layer with no signs of reconstruction, which makes the adatom version very unlikely.

Since the superstructure of rows forms on top of a substrate with fourfold symmetry, two domains rotated by  $90^\circ$  with respect to each other are likely to be observed. In LEED patterns, indeed, both domains always occur. From the spot profiles' half-width one can estimate a domain size of at least  $100 \text{ \AA}$ . On the (100) terrace of the FIM tip of about  $35 \text{ \AA}$  in diameter only one domain is observed (Fig. 1). After complete field evaporation of the topmost layer, during which rows  $\alpha$  and  $\beta$  are removed simultaneously, and after subsequent annealing at  $T > 900 \text{ K}$  in intervals of several seconds, either orientation of the domains develops with equal probability on the same tip (Fig. 4).

In accordance with LEED observations by Heinz *et*

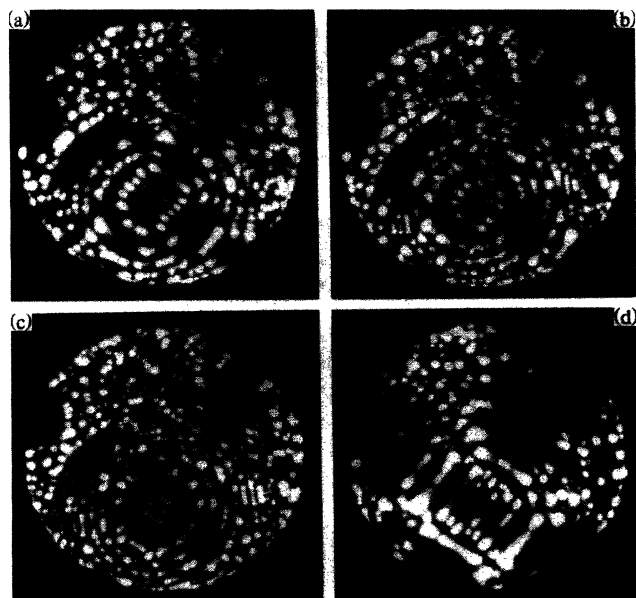


FIG. 4. Observation of different superstructure domain orientations. Starting with the terrace of Fig. 1, the images (a)–(c) show different stages after stepwise field evaporation; (d) is the image after subsequent annealing at 1200 K.

of this laboratory<sup>3</sup> the nonreconstructed ( $1\times 1$ ) phase can be prepared also on the tip by deliberate  $O_2$  adsorption (or adsorption from the residual gas) and subsequent annealing at 700 K. By this treatment at least part of the oxygen remains on the surface. It will subsequently be removed under the influence of the imaging field, which leaves the clean metastable ( $1\times 1$ ) structure exposed. Annealing at elevated temperatures, as described in the beginning, restores the reconstructed phase. The appearance of its FIM image as well as the details of the transition between the stable and the metastable phases justifies the assumption that it is the Ir(100) reconstruction which has been observed in the field-ion microscope. The atomic positions determined from the image support the structure model already developed by LEED and other methods. Although no direct analysis of the tip's cleanliness was possible, we believe that no contaminants were present to affect the surface during its activation to the reconstructed phase. According to LEED experience with Ir samples the reconstructed surface appears as a clean phase while contaminants tend to turn its structure into the nonreconstructed phase.

Finally, Fig. 5 displays FIM images of several stages before, during, and after the formation of the reconstructed (100) phase. Among other faces Fig. 5(a) contains (110) and (113) terraces both of which appear in their reconstructed ( $1\times 2$ ) modification due to a

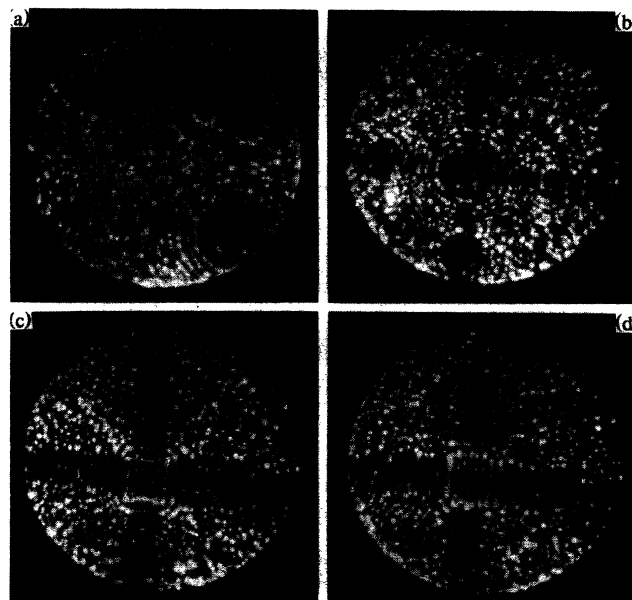


FIG. 5. (a) Reconstruction of  $(110)(1\times 2)$  and  $(113)(1\times 2)$ ; no indications for unusual structure at (100). (b)–(d) The same (100) face after annealing of the tip at (b) 900, (c) 1100, and (d)  $> 1200$  K for 20 sec each.

preceding heat treatment followed by incomplete field evaporation. The (100) face, however, shows no significant appearance and represents presumably the bulklike ( $1\times 1$ ) structure. For the following photographs the image is centered at the (100) terrace. After heating at  $T_1 = 900$  K for 20 sec rows of atoms appear [Fig. 5(b)] which can move (not shown in the photograph) on the nonresolved substrate. Heating at  $T_2 = 1100$  K for another period of 20 sec with the imaging field cut off results in the formation of double rows [Fig. 5(c)]. Final annealing at  $T_3 > 1200$  K produces the fully developed reconstructed surface [Fig. 5(d)] which has already been discussed above.

Future experiments with the field-ion microscope can be expected to reveal more detailed information on the interaction between atoms and between rows of atoms in viewing of the process of reconstruction.

Financial support by Deutsche Forschungsgemeinschaft is gratefully acknowledged.

<sup>1</sup>A. J. Melmed, R. T. Tung, W. R. Graham, and G. D. W. Smith, Phys. Rev. Lett. **43**, 1521 (1979).

<sup>2</sup>G. L. Kellogg, Phys. Rev. Lett. **55**, 2186 (1985).

<sup>3</sup>K. Heinz, G. Schmidt, L. Hammer, and K. Müller, Phys. Rev. B **32**, 6214 (1985).

<sup>4</sup>E. Lang, K. Müller, K. Heinz, M. A. Van Hove, R. J. Koestner, and G. A. Somorjai, Surf. Sci. **127**, 347 (1983); W. Moritz, Habilitationsschrift, Universität München, 1984

(unpublished); N. Bickel and K. Heinz, *Surf. Sci.* **163**, 435 (1985).

<sup>5</sup>D. W. Bassett, in *Surface Mobilities on Solid Materials*, edited by V. Th. Binh (Plenum, New York, 1983), pp. 83-108.

<sup>6</sup>K. Heinz and K. Müller, in *Structural Studies of Surfaces*, edited by G. Höhler, Springer Tracts in Modern Physics Vol.

91 (Springer-Verlag, Berlin, 1982), p. 1.

<sup>7</sup>Herbert H. H. Homeier and D. R. Kingham, *J. Phys. D* **16**, L115 (1983); J. Witt and K. Müller, *J. Phys. (Paris), Colloq.* **47**, C2-465 (1986).

<sup>8</sup>M. A. Van Hove, R. J. Koestner, P. C. Stair, J. P. Bibérian, L. L. Kesmodel, I. Bartos, and G. A. Somorjai, *Surf. Sci.* **103**, 189 (1981).

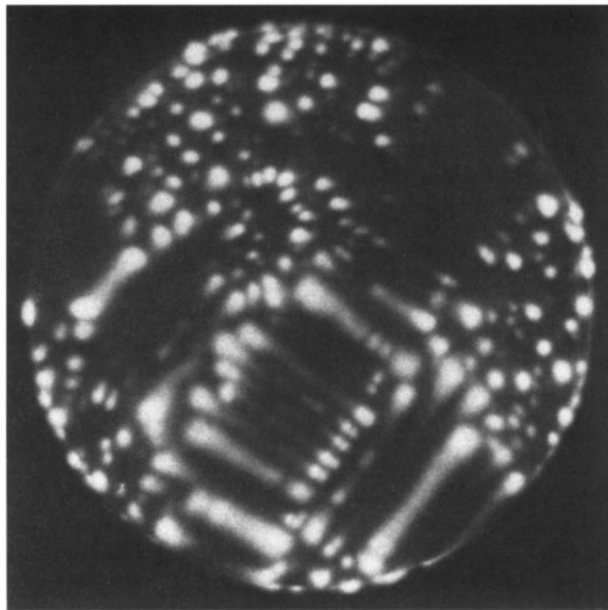


FIG. 1. FIM image of the Ir(100) plane after flashing of the tip to about 1500 K.

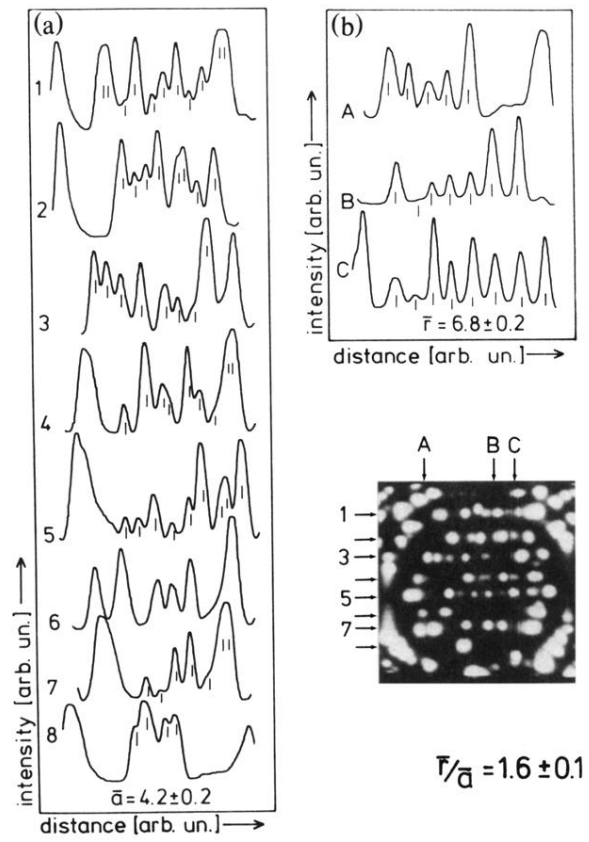


FIG. 2. Intensity profiles along (left-hand panel) and across (right-hand panel) rows taken from the FIM image shown at the lower right.

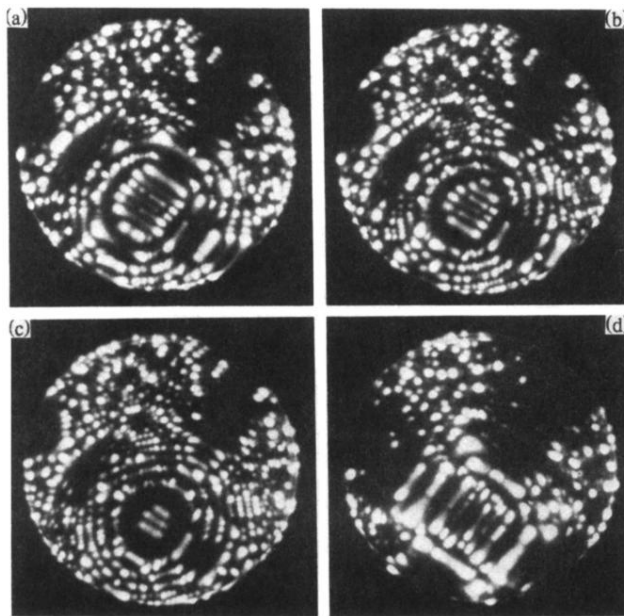


FIG. 4. Observation of different superstructure domain orientations. Starting with the terrace of Fig. 1, the images (a)–(c) show different stages after stepwise field evaporation; (d) is the image after subsequent annealing at 1200 K.

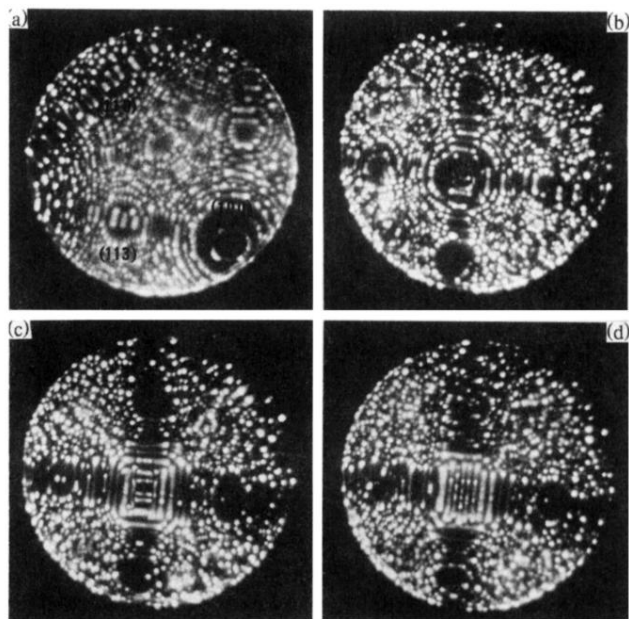


FIG. 5. (a) Reconstruction of  $(110)(1 \times 2)$  and  $(113)(1 \times 2)$ ; no indications for unusual structure at  $(100)$ . (b)–(d) The same  $(100)$  face after annealing of the tip at (b) 900, (c) 1100, and (d)  $>1200$  K for 20 sec each.